# Metallomics

Check for updates

# Hierarchical binding of copper$^{II}$ to N-truncated Aβ$_{4-16}$ peptide†

Xiangyu Teng, [iD] ‡[a] Ewelina Stefaniak, [iD] ‡[b] Paul Girvan, [iD] [a] Radosław Kotuniak, [iD] [b] Dawid Płonka, [iD] [b] Wojciech Bal [iD] *[b] and Liming Ying [iD] *[c]

**N-Truncated Aβ$_{4-42}$ displays a high binding affinity with Cu$^{II}$. A mechanistic scheme of the interactions between Aβ$_{4-42}$ and Cu$^{II}$ has been proposed using a fluorescence approach. The timescales of different conversion steps were determined. This kinetic mechanism indicates the potential synaptic functions of Aβ$_{4-42}$ during neurotransmission.**

The amyloid-β (Aβ) peptides associated with Alzheimer's Disease (AD) comprise a number of species. The "canonical" Aβ$_{1-42}$ and Aβ$_{1-40}$ peptides derived directly by proteolysis of the Amyloid Precursor Protein (APP) are complemented by N- and C-truncated species, yielded by a variety of brain proteases.[1] Among them, the N-truncated Aβ$_{4-42}$ has been reported as particularly abundant in the hippocampus and cortex of sporadic AD patients, as well as in healthy controls,[2,3] even exceeding Aβ$_{1-42}$ and Aβ$_{1-40}$.[4,5] Aβ$_{1-x}$ peptides can bind Cu$^{II}$ using the N-terminus and H6, H13, and His14 residues.[6–8] Hence, Aβ$_{1-16}$ has been adopted as a common model peptide in metal binding studies. $K_d$ in the range of 0.1 nM to 1 nM at pH 7.1–7.4 was determined for Aβ$_{1-16}$ and Aβ$_{1-40}$.[9–11] The adventitious binding of Cu$^{II}$ ions to Aβ$_{1-42/40}$ and the concomitant generation of reactive oxygen species (ROS) via the Cu$^{II}$/Cu$^I$ redox pair has been proposed to be the molecular basis of oxidative stress and neuronal death in AD.[12] On the other hand, Aβ$_{4-x}$ peptides bind a Cu$^{II}$ ion more than three orders of magnitude more strongly ($K_d$ = 30 fM and 6.6 fM at pH 7.4 for Aβ$_{4-16}$ and Aβ$_{4-9}$, respectively), using their N-terminal ATCUN motif spanning the Phe4, Arg5 and His6 residues. These complexes are redox-inert and do not generate significant ROS. Cu$^{II}$ ion transfer from Aβ$_{1-16}$ to Aβ$_{4-16}$ occurs upon adding the latter to the Cu$^{II}$Aβ$_{1-16}$ solution.[13]

[a] *Department of Chemistry, Imperial College London, Molecular Sciences Research Hub, White City Campus, London W12 0BZ, UK*

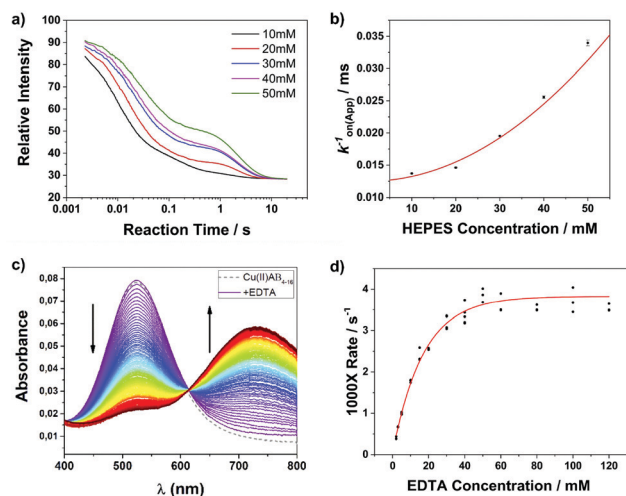[b] *Institute of Biochemistry and Biophysics, Polish Academy of Sciences, Pawińskiego 5a, 02-106 Warsaw, Poland. E-mail: wbal@ibb.waw.pl*

[c] *National Heart and Lung Institute, Imperial College London, Molecular Sciences Research Hub, White City Campus, London W12 0BZ, UK.*
*E-mail: l.ying@imperial.ac.uk*

† Electronic supplementary information (ESI) available. See DOI: 10.1039/c9mt00299e
‡ These authors contributed equally to this work.

## Significance to metallomics

N-Truncated Aβ$_{4-x}$ is abundant in both healthy and AD brains. Its Cu(II) binding affinity is three orders of magnitude stronger than well-known Aβ$_{1-42}$ or Aβ$_{1-40}$. Using a model peptide, Aβ$_{4-16}$, we have elucidated the reaction mechanism of Cu(II) with Aβ$_{4-x}$, crucial to understand the physiological role and toxicity of Aβ peptides. The presence of two kinetic intermediates prior to the formation of the tight ATCUN complex has implications for the potential function of Aβ$_{4-42}$ as a Cu(II) transporter during neurotransmission. The methodology used in this work may also stimulate the research of Cu(II) interactions with other intrinsically disordered proteins (IDPs).

This reaction is quantitative, in agreement with the affinity difference, and fast, occurring within the sample preparation time ∼s. Such a reaction suggested that Aβ$_{4-42}$ should prevail as a Cu$^{II}$ binding Aβ species in the extracellular spaces of the brain. This finding gave rise to a hypothesis that Aβ$_{4-42}$ may have a physiological role as a synaptic Cu$^{II}$ scavenger during neurotransmission.[14] However, Cu$^{II}$ release events in glutamatergic synapses may occur on a much faster, millisecond scale. Therefore, a thorough determination of association and dissociation rate constants for the participating species is necessary to help evaluate their relevance *in vivo*. Such data have been obtained previously for Cu$^{II}$Aβ$_{1-x}$ complexes.[15–17] Here, we studied the reaction mechanism for Cu$^{II}$ binding to the model peptide Aβ$_{4-16}$ and found that the reaction follows a hierarchical fashion, going through two intermediate states and then reaching the final tight complex.

First, we studied the effect of N-truncation on the Cu$^{II}$ binding kinetics. 20 nM Aβ labelled by HiLyte Fluor 488 on lysine 16 (FRHDSGYEVHHQK-HiLyte 488) was reacted with 400 nM Cu$^{II}$ under various HEPES concentrations in order to obtain the HEPES-independent Cu$^{II}$ binding rate constant ($k_{on}$). The results are shown in Fig. 1a. The intercept of the fitted curve (Fig. 1b) was used to determine $k_{on}$, which is $2.0(1) \times 10^8$ M$^{-1}$ s$^{-1}$, 2.5 times slower than the value for Aβ$_{1-16}$.[17]

$k_{off}$ was determined for the reaction of a Cu$^{II}$ complex of unlabelled Aβ$_{4-16}$ with an excess of EDTA. The estimated value

**Fig. 1** Kinetics of $Cu^{II}$ binding to $A\beta_{4-16}$. (a) Representative raw traces of $A\beta$ (20 nM) with $Cu^{II}$ (400 nM) under various concentrations of HEPES. The experiments were performed in 50 mM HEPES and 100 mM NaCl buffer solution at 298 K (pH 7.5). (b) HEPES dependence of $k_{on}$. The HEPES independent $k_{on}$ value is $2.0(1) \times 10^8$ $M^{-1}$ $s^{-1}$. (c) Kinetics of dissociation of $Cu^{II}A\beta_{4-16}$ assisted by varying concentrations of EDTA, monitored by UV-vis absorbance. The experiments were performed for 1 mM $Cu^{II}A\beta_{4-16}$ at 298 K (pH 7.5). (d) Empirical fit to derive the EDTA-independent $k_{off}$.

is $\sim 5 \times 10^{-5}$ $s^{-1}$, which divided by $k_{on}$ proposed here gives $K_d \sim 250$ fM. EDTA is a stronger $Cu^{II}$ chelator than $A\beta_{4-16}$, with a $\log \beta$ of 18.7, which can be recalculated into a conditional constant $^CK$ of 16.0 at pH 7.5.[18] This value is sufficiently higher than that of $Cu^{II}A\beta_{4-16}$, 13.53, to assure full $Cu^{II}$ transfer, as demonstrated in Fig. 1c. The reaction was carried out for a range of EDTA/peptide ratios between 2 and 120. Pseudo-1st order kinetics for the $Cu^{II}$ transfer reaction was observed for all experiments. The non-linear response of $k_{off}$ to EDTA required the EDTA-independent $k_{off}$ value to be determined by the extrapolation of the empirical exponential fit to these data, as shown in Fig. 1d.

To gain a glimpse of a possible reaction mechanism of $Cu^{II}$ binding to N-truncated $A\beta_{4-16}$, we performed binding experiments at a 1:1 mixing ratio of $A\beta$ to $Cu^{II}$ with increasing concentration. In such experiments, the effect of the second $Cu^{II}$ binding can be ignored, as the relevant $\log K$ is as low as 6.7.[13] The raw traces are shown in Fig. 2a. We noticed that the reaction process is becoming concentration independent after $\sim 2$ s (results from the fit are summarized in Table S1, ESI†). Thus we infer the existence of an intramolecular process following the initial $Cu^{II}$ binding.

Next, a double mixing stopped flow technique was employed to further explore the potential intermediate complexes formed after the initial $Cu^{II}$ binding. This technique was successfully applied to probe the interconversion between component I and component II $Cu^{II}$ coordination species of $A\beta_{1-16}$ and $A\beta_{1-40}$.[17] 2 μM $A\beta_{4-16}$ and 2 μM $Cu^{II}$ were mixed in a delay loop and after various delay times the reaction was "frozen" by adding an excess of EDTA (Fig. 2b). Taking advantage of the disparities in reactivity of different $Cu^{II}A\beta_{4-16}$ species with EDTA, the time evolution of the population of individual species could be
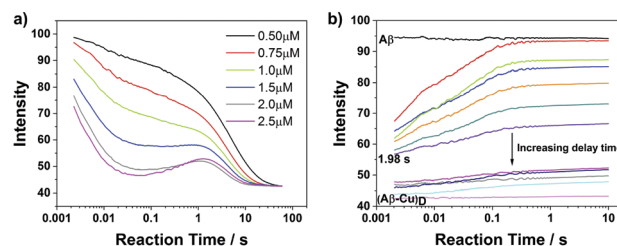


**Fig. 2** (a) Raw traces of $Cu^{II}$ binding measurements with a series of 1:1 concentration ratio HiLyte 488 labelled $A\beta$ and $Cu^{II}$ showing the evidence of intermediate species formation. The experiment was performed in 50 mM HEPES and 100 mM NaCl buffer solution at 298 K (pH 7.5). (b) Kinetics of HiLyte 488 labelled $A\beta/Cu^{II}$ interactions measured by double mixing stopped flow. Raw traces showing the change in amplitude as the delay time between mixing of an equal concentration of $Cu^{II}$ and $A\beta$ (2 μM) and addition of EDTA is increased from 50 ms to 1 min. The experiment was performed in 50 mM HEPES and 100 mM NaCl buffer solution at 298 K (pH 7.5).

resolved and analyzed, enabling us to depict details of the binding process.

As shown in Fig. 2b, the amplitude of fluorescence recovery strongly depends on the delay time, indicating that a much more inert (less reactive towards EDTA) complex ("dark" complex) formed after around 2 s. We equate this end complex, $(A\beta-Cu)_D$, to the very stable ATCUN-type $Cu^{II}A\beta_{4-16}$ complex reported previously.[13] Furthermore, because the reaction rate is concentration independent after 2 s as mentioned above, we propose that a peptide conformational rearrangement process leading to this final complex must occur at around 2 s.

In order to describe the whole process of $Cu^{II}$ binding of N-truncated $A\beta_{4-16}$, we hypothesized a reaction scheme as shown in Fig. 3a. The individual amplitudes of the two phases in Fig. 2b were determined by a global fit, which were further fitted by the scheme with KinTek software to validate it (Fig. 3b). The amplitudes indicate the amounts of two intermediates, Species I and Species II, at different reaction process stages, and could be
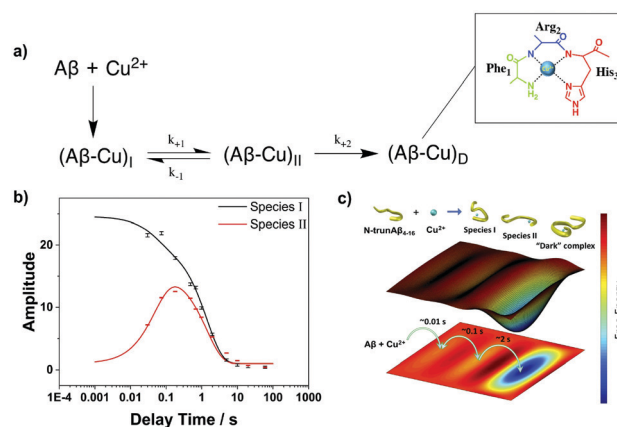


**Fig. 3** (a) Reaction mechanism of $Cu^{II}$ binding to $A\beta_{4-16}$ and formation of the high affinity $Cu^{II}A\beta_{4-16}$ complex, $(A\beta-Cu)_D$ ($Cu^{II}$ binding site shown above). (b) Fitting of the individual amplitudes at different $Cu^{II}$ binding process stages of the two phases by the predicted reaction mechanism. (c) Proposed free energy landscape of $Cu^{II}$ binding to $A\beta_{4-16}$. "Dark" complex refers to the very stable ATCUN-type $Cu^{II}A\beta_{4-16}$ complex.

Table 1 Rate constants corresponding to the mechanism scheme shown in Fig. 3a

|  | $k_{+1}$ | $k_{-1}$ | $k_{+2}$ |
|---|---|---|---|
| $k$ value/s$^{-1}$ | 4.10(1) | 10.34(2) | 3.31(4) |
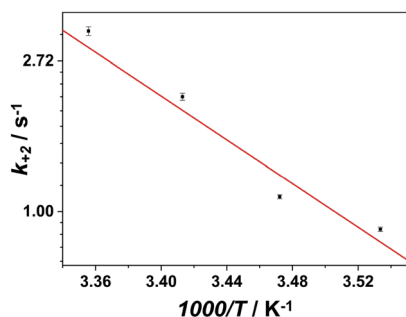


Fig. 4 Arrhenius plot for the switching rate constant $k_{+2}$. The switching activation energy determined is 64(3) kJ mol$^{-1}$.

fitted well by the predicted mechanism, with fitted rate constants listed in Table 1. A corresponding free energy landscape illustration of Cu$^{II}$ binding with A$\beta_{4-16}$ is shown in Fig. 3c.

Finally, the activation energy of the (A$\beta$–Cu)$_D$ complex was determined to be 64(3) kJ mol$^{-1}$ (Fig. 4) by performing a series of double mixing experiments at different temperatures (raw data shown in Fig. S1, ESI†).

The chemical properties of ATCUN Cu$^{II}$ complexes of A$\beta_{4-x}$ peptides, such as high thermodynamic stability, absence of ROS production due to their resistance to oxidation and reduction, reluctance of copper to transfer to metallothionein-3 (MT3) and easy sequestering of Cu$^{II}$ from A$\beta_{1-x}$, gave rise to a concept that A$\beta_{4-x}$ peptides (full-length A$\beta_{4-42}$ and its C-truncated analogs) may serve as guardians of synaptic function, by sequestering excess Cu$^{II}$ ions released during neurotransmission in glutamatergic pathways.[14,19] The key unsolved issue is how these exchange-inert complexes relay copper back to neurons to maintain the proper copper cycling. Furthermore, Cu$^{II}$-free A$\beta_{4-42}$ can be neurotoxic by forming oligomeric species.[20] Detailed knowledge on mechanisms of Cu$^{II}$ association with and dissociation from A$\beta_{4-x}$ peptides, represented here by A$\beta_{4-16}$, is thus crucial to understand the physiology and toxicity of these A$\beta$ peptides.

The discovery of long-lived kinetic intermediates in the formation of the ATCUN complex of A$\beta_{4-16}$ is a game changer in the above considerations. The lifetimes of Species I and Species II complexes are comparable to the intervals between pulses of neurotransmitter release in glutamatergic neuronal pathways.[21] Therefore, these complexes may well contribute to the biological activity of A$\beta_{4-42}$, and of putative short peptidic fragments generated by neprilysin cleavage, such as A$\beta_{4-9}$.[22,23] There is only one way in which four nitrogen ligands of the ATCUN motif can be arranged around the Cu$^{II}$ ion, and so it is reasonable to assume that the intermediate species contain the coordinatively unsaturated Cu$^{II}$. Such species have been implicated in the reverse reaction of Cu$^{II}$ dissociative transfer from Cu$^{II}$A$\beta_{4-16}$ to MT3, to explain the catalytic effect of glutamate,[24]

but it has not been observed directly. The Species I and in particular the longer-lived Species II complex may be the actual species able to move copper around during neurotransmission. The fact that the Cu$^{II}$A$\beta_{1-x}$ complex, although so much weaker, was formed 2.5 times faster, prompts further research into possible synaptic roles of Cu$^{II}$ interactions with various A$\beta$ species.

Furthermore, the observed hierarchical binding of Cu$^{II}$ to A$\beta_{4-16}$ resembles the kinetics of the binding of many intrinsically disordered proteins (IDPs).[25] The methodology used in this study may be applicable to the fundamental understanding of the emerging "coupled binding and folding" paradigm.[26]

## Conflicts of interest

There are no conflicts to declare.

## Acknowledgements

## Notes and references

1 D. J. Selkoe, *Physiol. Rev.*, 2001, **81**, 741–766.
2 C. L. Masters, G. Simms, N. A. Weinman, G. Multhaup, B. L. McDonald and K. Beyreuther, *Proc. Natl. Acad. Sci. U. S. A.*, 1985, **82**, 4245–4249.
3 E. Portelius, N. Bogdanovic, M. K. Gustavsson, I. Volkmann, G. Brinkmalm, H. Zetterberg, B. Winblad and K. Blennow, *Acta Neuropathol.*, 2010, **120**, 185–193.
4 G. Antonios, N. Saiepour, Y. Bouter, B. C. Richard, A. Paetau, A. Verkkoniemi-Ahola, L. Lannfelt, M. Ingelsson, G. G. Kovacs, T. Pillot, O. Wirths and T. A. Bayer, *Acta Neuropathol. Commun.*, 2013, **1**, 56.
5 T. A. Bayer and O. Wirths, *Acta Neuropathol.*, 2014, **127**, 787–801.
6 P. Dorlet, S. Gambarelli, P. Faller and C. Hureau, *Angew. Chem.*, 2009, **121**, 9437–9440 (*Angew. Chem., Int. Ed.*, 2009, **48**, 9273–9276).
7 B. Alies, H. Eury, C. Bijani, L. Rechignat, P. Faller and C. Hureau, *Inorg. Chem.*, 2011, **50**, 11192–11201.
8 E. Atrián-Blasco, P. Gonzalez, A. Santoro, B. Alies, P. Faller and C. Hureau, *Coord. Chem. Rev.*, 2018, **375**, 38–55.
9 B. Alies, E. Renaglia, M. Rózga, W. Bal, P. Faller and C. Hureau, *Anal. Chem.*, 2013, **85**, 1501–1508.
10 T. R. Young, A. Kirchner, A. G. Wedd and Z. Xiao, *Metallomics*, 2014, **6**, 505–517.

11  A. Conte-Daban, V. Borghesani, S. Sayen, E. Guillon, Y. Journaux, G. Gontard, L. Lisnard and C. Hureau, *Anal. Chem.*, 2017, **89**, 2155–2162.

12  C. Cheignon, M. Jones, E. Atrián-Blasco, I. Kieffer, P. Faller, F. Collin and C. Hureau, *Chem. Sci.*, 2017, **8**, 5107–5118.

13  M. Mital, N. E. Wezynfeld, T. Frączyk, M. Z. Wiloch, U. E. Wawrzyniak, A. Bonna, C. Tumpach, K. J. Barnham, C. L. Haigh, W. Bal and S. C. Drew, *Angew. Chem.*, 2015, **127**, 10606–10610 (*Angew. Chem., Int. Ed.*, 2015, **54**, 10460–10464).

14  E. Stefaniak and W. Bal, *Inorg. Chem.*, 2019, **58**, 13561–13577.

15  P. Girvan, T. Miyake, X. Teng, T. Branch and L. Ying, *ChemBioChem*, 2016, **17**, 1732–1737.

16  T. Branch, M. Barahona, C. A. Dodson and L. Ying, *ACS Chem. Neurosci.*, 2017, **8**, 1970–1979.

17  T. Branch, P. Girvan, M. Barahona and L. Ying, *Angew. Chem.*, 2015, **127**, 1243–1246 (*Angew. Chem., Int. Ed.*, 2015, **54**, 1227–1230).

18  J. Felcman and J. J. da Silva, *Talanta*, 1983, **30**, 565–570.

19  N. E. Wezynfeld, E. Stefaniak, K. Stachucy, A. Drozd, D. Płonka, S. C. Drew, A. Krężel and W. Bal, *Angew. Chem.*, 2016, **128**, 8375–8378 (*Angew. Chem., Int. Ed.*, 2016, **55**, 8235–8238).

20  J. Dunys, A. Valverde and F. Checler, *J. Biol. Chem.*, 2018, **293**, 15419–15428.

21  W. Goch and W. Bal, *PLoS One*, 2017, **12**, e0170749.

22  M. Mital, W. Bal, T. Frączyk and S. C. Drew, *Inorg. Chem.*, 2018, **57**, 6193–6197.

23  K. Bossak-Ahmad, M. Mital, D. Płonka, S. C. Drew and W. Bal, *Inorg. Chem.*, 2019, **58**, 932–943.

24  A. Santoro, N. Wezynfeld, E. Stefaniak, A. Pomorski, D. Płonka, A. Krezel, W. Bal and P. Faller, *Chem. Commun.*, 2018, **54**, 12634–12637.

25  K. Sugase, H. J. Dyson and P. E. Wright, *Nature*, 2007, **447**, 1021–1025.

26  S. Gianni, J. Dogan and P. Jemth, *Curr. Opin. Struct. Biol.*, 2016, **36**, 18–24.